Low Thermal Resistances at GaN–SiC Interfaces for HEMT Technology

Jungwan Cho, Elah Bozorg-Grayeli, David H. Altman, Mehdi Asheghi, and Kenneth E. Goodson

***Abstract*—The temperature rise in AlGaN/GaN high-electron-mobility transistors depends strongly on the GaN-substrate thermal interface resistance (TIR). We apply picosecond time-domain thermoreflectance measurements to GaN-SiC composite substrates with varying GaN thickness to extract both the TIR and the intrinsic GaN thermal conductivity at room temperature. Two complementary data extraction methodologies yield 4–5 $m^2 \cdot K/GW$ for the GaN-SiC TIR and 157–182 $W/m \cdot K$ for the GaN conductivity. The GaN-SiC interface resistance values reported here, as well as the TIR experimental uncertainties documented in this letter, are substantially lower than those reported previously for this material combination.**

***Index Terms*—AlGaN/GaN high-electron-mobility transistors (HEMTs), picosecond pump–probe thermometry, thermal conductivity, thermal interface resistance (TIR).**

I. Introduction

HIGH-electron-mobility transistors (HEMTs) based on AlGaN/GaN are promising because of their high-power and high-frequency capabilities [1]. However, device-level self-heating limits the peak power density [2]. The low thermal conductivity of the GaN buffer layer and the high thermal resistances of interfaces in the composite substrates impede heat conduction. Past work estimated the thermal resistance at the GaN-substrate interface using either optical transient interferometric mapping [3] or Raman thermometry [3]–[5]. These measurements did not determine the GaN thermal conductivity but rather assumed a value for this property as an input to the data-fitting procedure. While the relevant through-plane thermal conductivity of representative GaN films has been measured accurately using the 3ω method [6], this property varies strongly with fabrication details. The community needs more accurate data and measurement strategies for the GaN conductivity and interface resistance, and these properties should be captured simultaneously in the same composite substrate targeted for HEMT applications. In this letter, we extract both the intrinsic GaN thermal conductivity and the GaN-SiC thermal interface resistance (TIR) at room temperature using picosecond pump-probe time-domain thermoreflectance (TDTR) thermometry.

TABLE I
Geometries and Thicknesses for Different Samples

	Al Thickness [nm]	GaN Thickness [nm]	AlN Thickness [nm]
Sample A	53.9 ± 3.6	884 ± 8	27.8 ± 0.9
Sample B	56.5 ± 2.9	1271 ± 8	26.9 ± 1.2
Sample C	53.8 ± 3.0	1562 ± 6	26.2 ± 1.7

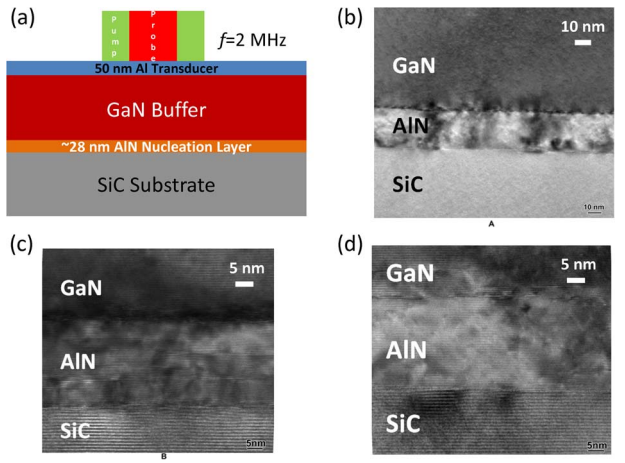

Fig. 1. (a) Cross-sectional schematic drawing of the GaN-on-SiC samples. Representative cross-sectional TEM images of (b) sample A, (c) sample B, and (d) sample C near the GaN-SiC interface with an ∼28-nm AlN nucleation layer.

II. Samples and Experimental Methods

The samples consist of three thicknesses of GaN on 4H–SiC wafers (Table I). The GaN epilayer was grown on a SiC substrate by metal–organic chemical vapor deposition (MOCVD) followed by dry etching to the target GaN thickness. An AlN nucleation layer (∼28 nm) between the GaN buffer and the SiC substrate minimizes lattice mismatch. An evaporated Al layer (50 nm thick) serves as the transducer for thermoreflectance measurements. Fig. 1 shows representative transmission electron microscopy (TEM) images for confirming sample dimensions. Microstructural defects are visible within the AlN nucleation layer and near its boundaries, and these hinder heat transport near the GaN-SiC interface due to increased phonon–defect scattering.

Manuscript received November 26, 2011; revised December 17, 2011; accepted December 19, 2011. Date of publication January 31, 2012; date of current version February 23, 2012. This work was supported by the Defense Advanced Research Projects Agency Microsystems Technology Office through Air Force Contract FA8650-10-7044. The work of J. Cho was supported in part by a Samsung Scholarship. The review of this letter was arranged by Editor J. A. del Alamo.

J. Cho, E. Bozorg-Grayeli, M. Asheghi, and K. E. Goodson are with the Department of Mechanical Engineering, Stanford University, Stanford, CA 94305-3030 USA (e-mail: suksak82@stanford.edu; ebozorgg@stanford.edu; mehdi@stanford.edu; goodson@stanford.edu).

D. H. Altman is with Raytheon Integrated Defense Systems, Sudbury, MA 01776 USA (e-mail: David_H_Altman@raytheon.com).

Color versions of one or more of the figures in this letter are available online at http://ieeexplore.ieee.org.

Digital Object Identifier 10.1109/LED.2011.2181481

0741-3106/$31.00 © 2012 IEEE

Picosecond TDTR is well established for determining thermal properties in multilayer thin-film structures [7]–[9]. A passively mode-locked Nd:YVO_4 laser with an 82-MHz repetition rate generates 9.2-ps pulses at wavelength $\lambda = 1064$ nm. A beam splitter separates these pulses into pump and probe components. The frequency-doubled pump beam, modulated at 2 MHz, deposits heat in the Al transducer. The probe beam is temporally delayed from the pump beam via a linear delay stage, and the beam determines the reflectivity of the transducer film. For small temperature rises, the reflected intensity measures the surface temperature decay over 3.5 ns [10]. A 3-D radial symmetric heat diffusion solution for the multilayer stack is fitted to the normalized temperature decay to extract the properties of films beneath the metal transducer [7]. We validate system accuracy by extracting a thermal conductivity of 1.38 $\mathrm{W/m \cdot K}$ for a SiO_2 calibration sample.

We are unable to resolve the intrinsic resistance of AlN (R_{AlN}) and the thermal boundary resistances (TBRs) at its boundaries ($TBR_{\mathrm{GaN-AlN}}$ and $TBR_{\mathrm{AlN-SiC}}$). Rather, we lump the three contributions into one single interface resistance: $TIR_{\mathrm{GaN-SiC}} = TBR_{\mathrm{GaN-AlN}} + R_{\mathrm{AlN}} + TBR_{\mathrm{AlN-SiC}}$. The thermal penetration depth of the modulated pump beam is approximately 2.1 μm in GaN, which is larger than the GaN layer thicknesses. As a result, the measurement is sensitive to both the GaN-SiC TIR $(TIR_{\mathrm{GaN-SiC}})$ and the GaN conductivity (k_{GaN}). We use multiple GaN thicknesses to extract the GaN conductivity and the TIR independently under the assumption that the properties do not vary strongly among the three samples.

We compare two methods for interpreting the thermal decay traces from the TDTR data: 1) a simultaneous fit of the TDTR temporal traces for all three samples and 2) extrapolation of the thermal resistances determined separately for the three samples. The first method optimizes the analytical thermal decay curves for all three samples to determine k_{GaN} and $TIR_{\mathrm{GaN-SiC}}$, with all other properties held constant. For the second method, we consider a single effective layer with conductivity k_{eff} that lumps k_{GaN} and $TIR_{\mathrm{GaN-SiC}}$ together. For thermal resistors in series, $L_{\mathrm{GaN}}/k_{\mathrm{eff}} = L_{\mathrm{GaN}}/k_{\mathrm{GaN}} + TIR_{\mathrm{GaN-SiC}}$, which shows that the stack resistance $(L_{\mathrm{GaN}}/k_{\mathrm{eff}})$ increases linearly with GaN thickness (L_{GaN}). A plot of stack resistance versus GaN thickness reveals k_{GaN} to be the inverse of the slope and $TIR_{\mathrm{GaN-SiC}}$ to be the y-intercept.

To accurately determine the properties of interest, all other thermal parameters must be known. The GaN and SiC heat capacities are taken from the literature [11], [12], a valid approach because these properties vary little with material quality for fully dense material. The SiC thermal conductivity and its conductivity anisotropy are measured using picosecond TDTR on the sample substrate without the GaN layer. To extract these properties, we utilize variable beamwidths for the SiC substrate coated with a 57-nm-thick Al film. By using a lower magnification objective, we widen the pump and probe beams (20-μm 1/e^2 pump diameter). A wider pump beam results in reduced sensitivity to radial losses, allowing unique extraction of cross-plane thermal conductivity. At room temperature, we find $k_{\mathrm{SiC,cross\text{-}plane}} = 390 \pm 45$ $\mathrm{W/m \cdot K}$ and $R_{\mathrm{Al-SiC}} = 8.2 \pm 0.6$ $\mathrm{m^2 \cdot K/GW}$. With a higher magnification objective (10-μm 1/e^2 pump diameter), the measurement becomes sensitive to in-plane SiC conductivity. Using the cross-plane conductivity taken from the previous measurement, we fit for the in-plane conductivity. Combining the best fit values for both measurements, the conductivity anisotropy $(\eta_{\mathrm{SiC}} = k_{\mathrm{SiC,in\text{-}plane}}/k_{\mathrm{SiC,cross\text{-}plane}})$ of the SiC substrate is estimated to be 0.58 ± 0.07. Here, the error bars are due to variation in the thickness of the Al transducer. Burgemeister *et al.* reported that the SiC thermal conductivity parallel to the c-axis is about 30% smaller than that in the direction normal to the c-axis for 6H–SiC, corresponding to $\eta_{\mathrm{SiC}} = 0.7$ [13]. The upper end of our measured value $(\eta_{\mathrm{SiC}} = 0.65)$ is consistent with this literature value considering experimental uncertainties.

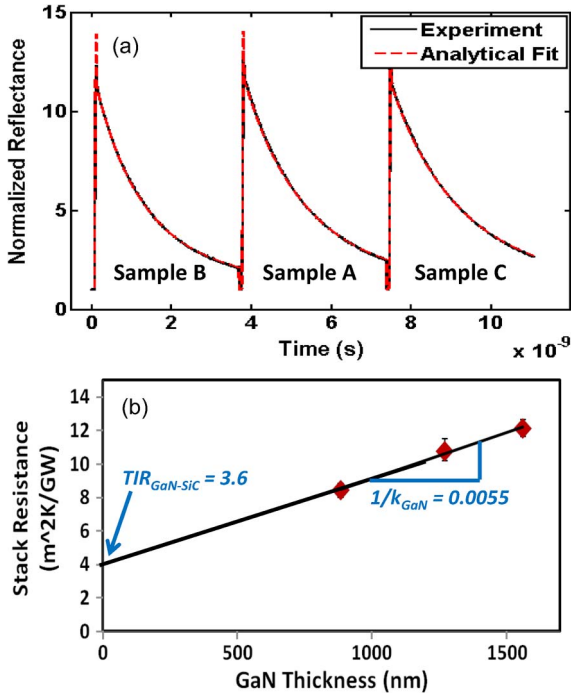

Fig. 2. (a) Simultaneous curve fits for all samples with representative thermal traces at 30 °C. (b) Plot of stack resistance versus GaN thickness. The slope indicates that the GaN conductivity is 182 $\mathrm{W/m \cdot K}$. The GaN-SiC TIR is 3.6 $\mathrm{m^2 \cdot K/GW}$ from the y-intercept.

III. Results and Discussion

Fig. 2 shows the two approaches described in Section II. Fig. 2(a) shows the simultaneous fitting approach for the representative thermal traces. Using this method, we find $k_{\mathrm{GaN}} = 157 \pm 11$ $\mathrm{W/m \cdot K}$ and $TIR_{\mathrm{GaN-SiC}} = 4.2 \pm 0.6$ $\mathrm{m^2 \cdot K/GW}$ at room temperature. Variations in the thickness of the Al transducer determine the error bars. Uncertainties due to multiple spot measurements lie within the error bars reported above. The initial time behavior (at time scales below $\sim$1 ns) of the thermal decay traces determines the Al–GaN TBRs, which vary between 8.9 and 13.3 $\mathrm{m^2 \cdot K/GW}$ for the three samples. The difference in the Al–GaN TBRs can be due to the different levels of oxidation, contamination, and roughness of the samples [9]. Regarding the second approach, a plot of stack resistance versus GaN thickness is shown in Fig. 2(b). Using this method, we obtain $k_{\mathrm{GaN}} = 182 \pm 33$ $\mathrm{W/m \cdot K}$ and $TIR_{\mathrm{GaN-SiC}} = 3.6 \pm 1.6$ $\mathrm{m^2 \cdot K/GW}$ within the error bars of

the previous technique. These GaN conductivities are comparable with existing published data [6].

Both the GaN-SiC interface resistances reported here and the uncertainty associated with these data are substantially lower than those reported previously. Manoi *et al.* [5] used micro Raman thermometry to extract GaN-SiC TIR values for ten different devices on GaN layers grown by MOCVD. These authors reported a TIR uncertainty of approximately 10 $\mathrm{m}^2 \cdot \mathrm{K/GW}$ (compared to $\sim$1 $\mathrm{m}^2 \cdot \mathrm{K/GW}$ in the current work) and did not measure the GaN conductivity. The TIR was strongly temperature dependent with increases of approximately 50% from 60 °C to 220 °C [5]. The lowest resistance reported in that study was 8 $\mathrm{m}^2 \cdot \mathrm{K/GW}$ at 110 °C to 18 $\mathrm{m}^2 \cdot \mathrm{K/GW}$ at 170 °C, which is comparable with the room-temperature resistances reported here considering the temperature dependence in the past work. The TIR values for the other nine samples in [5] extrapolate to much higher estimated room-temperature TIR values, which are 15–35 $\mathrm{m}^2 \cdot \mathrm{K/GW}$. While it is difficult to quantitatively estimate interface quality using TEM images, the lower TIR values reported in this work are almost certainly based on a lower defect density in the AlN transition layer.

Since phonons dominate heat transport in GaN films and at the GaN-SiC interface, the diffuse mismatch model (DMM) is a relevant theoretical model for predicting TBR at the AlN interfaces with GaN and with SiC. This model assumes that phonons are diffusely transmitted or reflected at the interface [14], [15]. The DMM resistance can be calculated using

$$R_b = \left(\frac{\Sigma_j c_{2,j}^{-2}}{12\left(\Sigma_j c_{1,j}^{-2} + \Sigma_j c_{2,j}^{-2}\right)} c_{1D}^3 \sum_j c_{1,j}^{-2} \right) C_1(T)^{-1} \quad (1)$$

where R_b is the TBR, $C_1(T)$ is the measured heat capacity of material 1 at temperature T, $c_{i,j}$ is the speed of sound through material i for the jth phonon mode, and c_{1D} is the average sound velocity in material 1 [15]. Phonon velocities in GaN, AlN, and SiC are taken from the literature [16]. DMM predicts a GaN–AlN TBR of 0.84–1.12 $\mathrm{m}^2 \cdot \mathrm{K/GW}$ and an AlN–SiC TBR of 0.53–0.59 $\mathrm{m}^2 \cdot \mathrm{K/GW}$. Taking our data for a 600-nm-thick AlN layer from an independent and unpublished study ($k_{\mathrm{AlN}} = 30.5$ $\mathrm{W/m \cdot K}$ at room temperature), the GaN–SiC TIR is estimated to be 2.3–2.6 $\mathrm{m}^2 \cdot \mathrm{K/GW}$ at room temperature using $TIR_{\mathrm{GaN-SiC}} = TBR_{\mathrm{GaN-AlN,DMM}} + R_{\mathrm{AlN}} + TBR_{\mathrm{AlN-SiC,DMM}}$. This prediction sets a lower limit for the measured resistance. Since AlN has better crystalline quality with increasing layer thickness [5], the $\sim$28-nm-thick AlN has lower thermal conductivity than the 600-nm-thick AlN. In addition, the real GaN-AlN and AlN-SiC TBRs can be larger than the DMM predictions due to increased phonon scattering by interfacial disorders such as grain boundaries, dislocations, impurities, and surface defects.

IV. Conclusion

The intrinsic GaN conductivity and the GaN-SiC TIR are extracted independently using picosecond TDTR. An extraction approach involving multiple GaN thicknesses leads to uncertainties much lower than that of the past work. The extracted GaN-SiC TIR is 4–5 $\mathrm{m}^2 \cdot \mathrm{K/GW}$, corresponding to $\sim$2 μm of SiC substrate. The equivalent SiC thickness of 2 μm is small compared to the total wafer thickness but can be significant as an extra resistance (with negligible thickness) presented in direct proximity to the heated device region. Spreading from a HEMT gate of width well below 1 μm will be influenced by this localized resistance, although the impact can be minimal depending on the power density of the transistor. The TIR determined here is the lowest reported for a GaN composite substrate, which is promising for HEMT thermal management.

References

[1] Y.-F. Wu, A. Saxler, M. Moore, P. Smith, S. Sheppard, M. Chavarkar, T. Wisleder, K. Mishra, and P. Parikh, "30 W/mm GaN HEMTs by field plate optimization," *IEEE Electron Device Lett.*, vol. 25, no. 3, pp. 117–119, Mar. 2004.

[2] G. Meneghesso, G. Verzellesi, F. Danesin, F. Rampazzo, F. Zanon, A. Tazzoli, M. Meneghini, and E. Zanoni, "Reliability of GaN high-electron-mobility transistors: State of the art and perspectives," *IEEE Trans. Device Mater. Rel.*, vol. 8, no. 2, pp. 332–343, Jun. 2008.

[3] J. Kuzmik, S. Bychikhin, D. Pogany, C. Gaquiere, E. Pichonat, and E. Morvan, "Investigation of the thermal boundary resistance at the III-nitride/substrate interface using optical methods," *J. Appl. Phys.*, vol. 101, no. 5, pp. 054508-1–054508-6, Mar. 2007.

[4] A. Sarua, H. Ji, P. Hilton, D. J. Wallis, J. Uren, T. Martin, and M. Kuball, "Thermal boundary resistance between GaN and substrate in AlGaN/GaN electronic devices," *IEEE Trans. Electron Devices*, vol. 54, no. 12, pp. 3152–3158, Dec. 2007.

[5] A. Manoi, J. W. Pomeroy, N. Killat, and M. Kuball, "Benchmarking of thermal boundary resistance in AlGaN/GaN HEMTs on SiC substrates: Implications of the nucleation layer microstructure," *IEEE Electron Device Lett.*, vol. 31, no. 12, pp. 1395–1397, Dec. 2010.

[6] W. Liu and A. A. Balandin, "Temperature dependence of thermal conductivity of $\mathrm{Al}_x\mathrm{Ga}_{1-x}\mathrm{N}$ thin films measured by the differential 3w technique," *Appl. Phys. Lett.*, vol. 85, no. 22, pp. 5230–5232, Nov. 2004.

[7] D. G. Cahill, "Analysis of heat flow in layered structures for time-domain thermoreflectance," *Rev. Sci. Instrum.*, vol. 75, no. 12, pp. 5119–5122, Nov. 2004.

[8] M. A. Panzer, M. Shandalov, J. A. Rowlette, Y. Oshima, Y. W. Chen, P. C. McIntyre, and K. E. Goodson, "Thermal properties of ultra-thin hafnium oxide gate dielectric films," *IEEE Electron Device Lett.*, vol. 30, no. 12, pp. 1269–1271, Dec. 2009.

[9] J. P. Reifenberg, K. W. Chang, M. Panzer, S. B. Kim, J. A. Rowlette, M. Asheghi, H. S. P. Wong, and K. E. Goodson, "Thermal boundary resistance measurements for phase-change memory devices," *IEEE Electron Device Lett.*, vol. 31, no. 1, pp. 56–58, Jan. 2010.

[10] K. Ujihara, "Reflectivity of metals at high temperature," *J. Appl. Phys.*, vol. 43, no. 5, pp. 2376–2383, May 1972.

[11] I. Zieborak-Tomaszkiewicz, E. Utzig, and P. Gierycz, "Heat capacity of crystalline GaN," *J. Therm. Anal. Cal.*, vol. 91, no. 1, pp. 329–332, Jan. 2008.

[12] L. Hitova, R. Yakimova, E. P. Trifonova, A. Lenchev, and E. Janzen, "Heat capacity of 4H–SiC determined by differential scanning calorimetry," *J. Electrochem. Soc.*, vol. 147, no. 9, pp. 3546–3547, Sep. 2000.

[13] E. A. Burgemeister, W. von Muench, and E. Pettenpaul, "Thermal conductivity and electrical properties of 6H silicon carbide," *J. Appl. Phys.*, vol. 50, no. 9, pp. 5790–5794, Sep. 1979.

[14] E. T. Swartz and R. O. Pohl, "Thermal boundary resistance," *Rev. Mod. Phys.*, vol. 61, no. 3, pp. 605–668, Jul. 1989.

[15] L. De Bellis, P. E. Phelan, and R. S. Prasher, "Variations of acoustic and diffuse mismatch models in predicting thermal-boundary resistance," *J. Thermophys. Heat Transf.*, vol. 14, no. 2, pp. 144–150, Apr.–Jun. 2000.

[16] M. Levinshtein, S. Rumyantsev, and M. Shur, *Properties of Advanced Semiconductor Materials: GaN, AlN, InN, BN, SiC, SiGe*. New York: Wiley, 2001.